Figures and figure supplements

RBP-J regulates homeostasis and function of circulating Ly6C^{lo} monocytes

Tiantian Kou and Lan Kang *et al*.

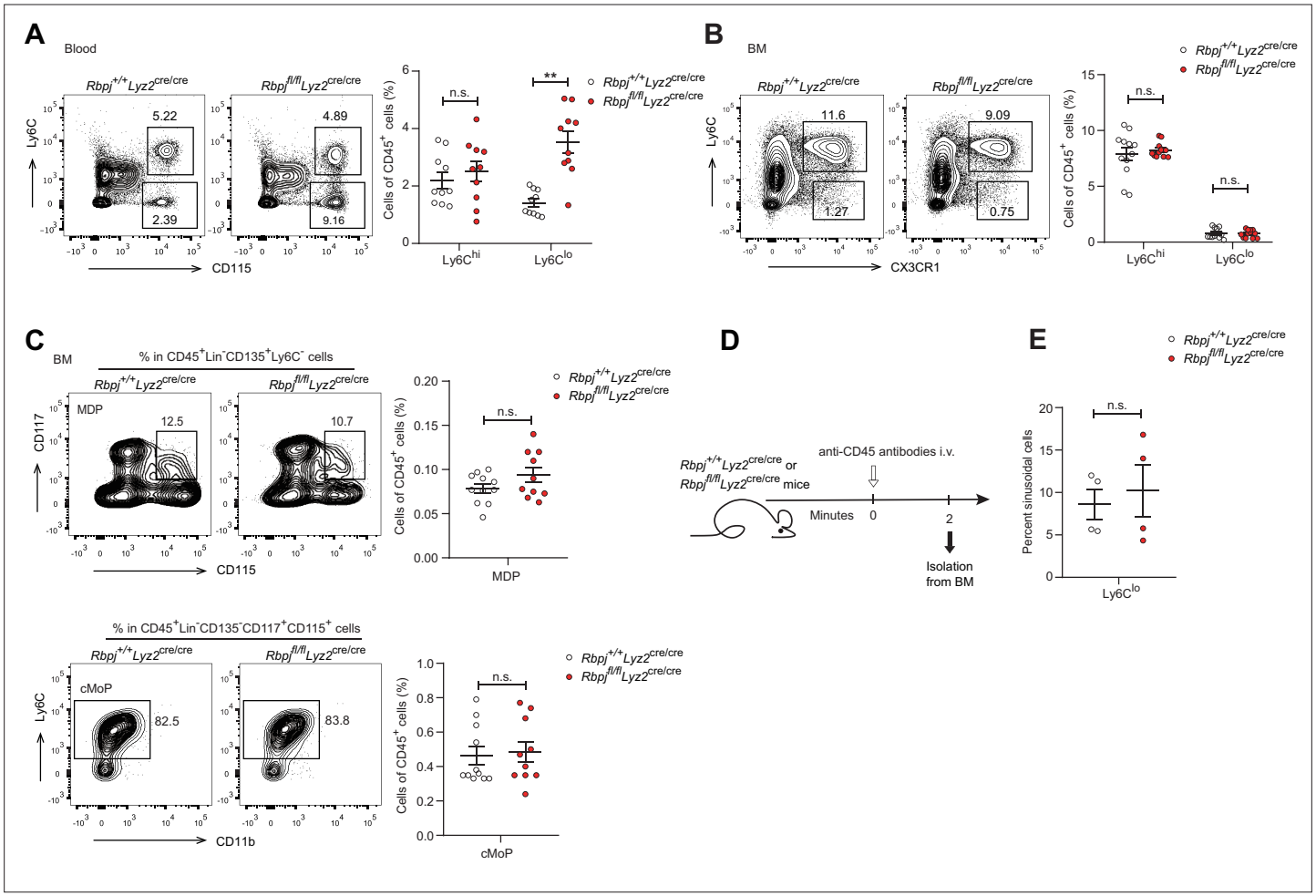

Figure 1. RBP-J-deficient mice display more blood Ly6C^{lo} monocytes. (**A**) Blood Ly6C^{hi} and Ly6C^{lo} monocytes in *Rbpj*$^{+/+}$*Lyz2*$^{cre/cre}$ control and *Rbpj*$^{fl/fl}$*Lyz2*$^{cre/cre}$ mice were determined by flow cytometry analyses (FACS). Representative FACS plots (left) and cumulative data of cell ratio (right) are shown. (**B, C**) Representative FACS plots and cumulative data quantitating percentages of bone marrow (BM) monocyte subsets (**B**) and myeloid progenitor cells (**C**) (CD45$^+$CD11b$^+$Ly6G$^-$CD115$^+$ Ly6C^{hi} monocyte; CD45$^+$CD11b$^+$Ly6G$^-$CD115$^+$Ly6C^{lo} monocyte; MDP, CD45$^+$Lin$^-$CD117$^+$CD115$^+$CD135$^+$ Ly6C$^-$; cMoP, CD45$^+$Lin$^-$CD11b$^-$CD117$^+$CD115$^+$ CD135$^-$Ly6C$^+$). Lin: CD3, B220, Ter119, Gr-1 and CD11b. (**D**) Experimental outline for panel (**E**). (**E**) Cumulative data quantitating percentages of sinusoidal monocytes (CD45$^+$) within total BM Ly6C^{lo} monocytes. Data are pooled from at least two independent experiments; n ≥ 4 in each group. Data are shown as mean ± SEM; n.s., not significant; **p<0.01 (two-tailed Student's unpaired *t*-test). Each symbol represents an individual mouse.

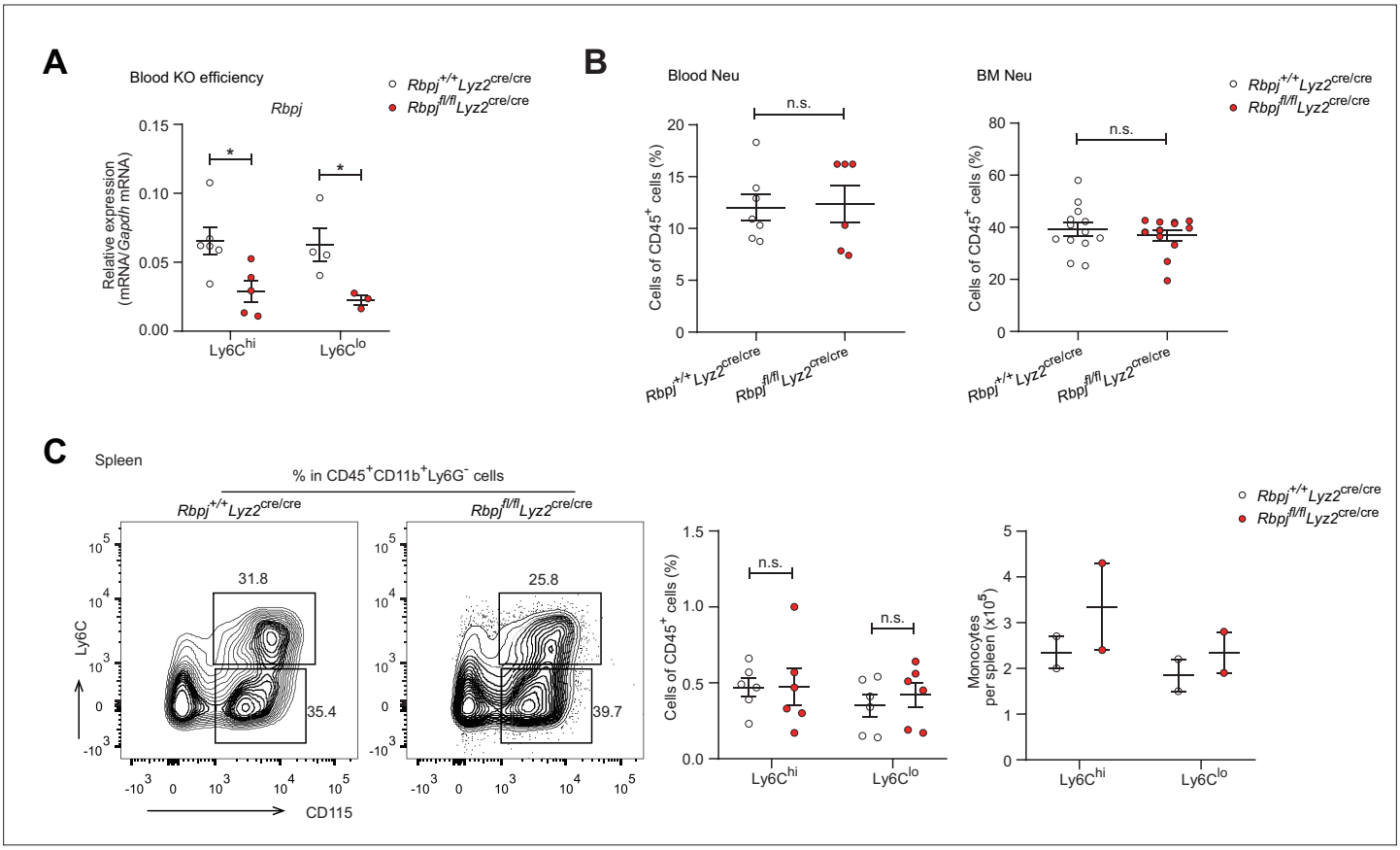

Figure 1—figure supplement 1. Control and RBP-J-deficient mice show similar neutrophils. (**A**) Quantitative real-time PCR (qPCR) analysis of *Rbpj* expression in sorted monocyte subsets from control and RBP-J-deficient mice. (**B**) Blood and bone marrow (BM) $CD45^+CD11b^+Ly6G^+$ neutrophils were determined by FACS. Cumulative data of cell ratio are shown. (**C**) Spleen monocyte subsets were determined by FACS. Representative FACS plots (left) and cumulative data of cell ratio and absolute numbers (right) are shown. Data are pooled from at least two independent experiments; n ≥ 2 in each group. Data are shown as mean ± SEM; n.s., not significant; *p<0.05 (two-tailed Student's unpaired *t*-test). Each symbol represents an individual mouse.

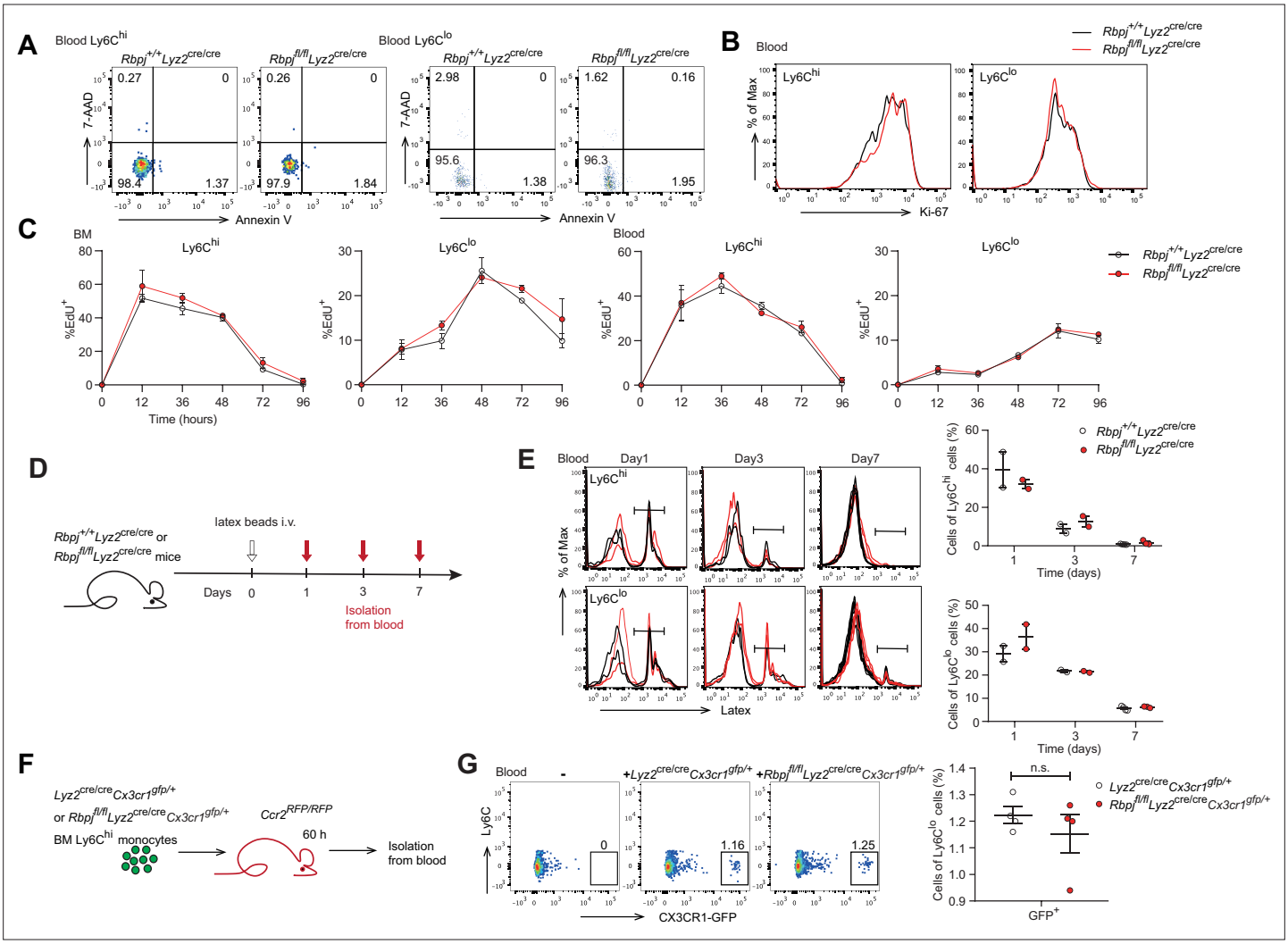

Figure 2. Monocyte subsets in RBP-J-deficient mice display normal cell death. (**A**) Representative FACS plots of monocyte subsets in blood stained with 7-amino-actinomycin D (7-AAD) and Annexin V. (**B**) FACS analysis of Ki-67 expression in *Rbpj*$^{+/+}$*Lyz2*$^{cre/cre}$ control and *Rbpj*$^{fl/fl}$*Lyz2*$^{cre/cre}$ blood monocyte subsets. Black lines represent control mice, and red lines represent RBP-J-deficient mice. (**C**) Analysis of time course of EdU incorporation of monocyte subsets in bone marrow (BM) and blood after a single 1 mg EdU pulsing. The percentages of EdU^{+} cells among the indicated monocyte subsets are shown. (**D**) Experimental outline for panel (**E**). (**E**) Analysis of time course of latex beads incorporation of monocyte subsets in blood after latex beads injection. The percentages of latex^{+} cells among the indicated monocyte subsets are shown. (**F**) Cartoon depicting the adoptive transfer. BM GFP^{+}Ly6C^{hi} monocytes were sorted from *Lyz2*$^{cre/cre}$*Cx3cr1*$^{gfp/+}$ or *Rbpj*$^{fl/fl}$*Lyz2*$^{cre/cre}$*Cx3cr1*$^{gfp/+}$ mice and transferred into *Ccr2*$^{RFP/RFP}$ recipient mice. Sixty hours after transfer, cell fate was analyzed. (**G**) Representative FACS plots are shown in the left panel, and the frequencies of GFP^{+}Ly6C^{lo} monocytes within total Ly6C^{lo} monocytes are shown in the right panel. Data are pooled from two independent experiments (**G**); n ≥ 2 in each group (**C, E, G**). Data are shown as mean ± SEM; n.s., not significant; (two-tailed Student's unpaired *t*-test). Each symbol represents an individual mouse (**E, G**).

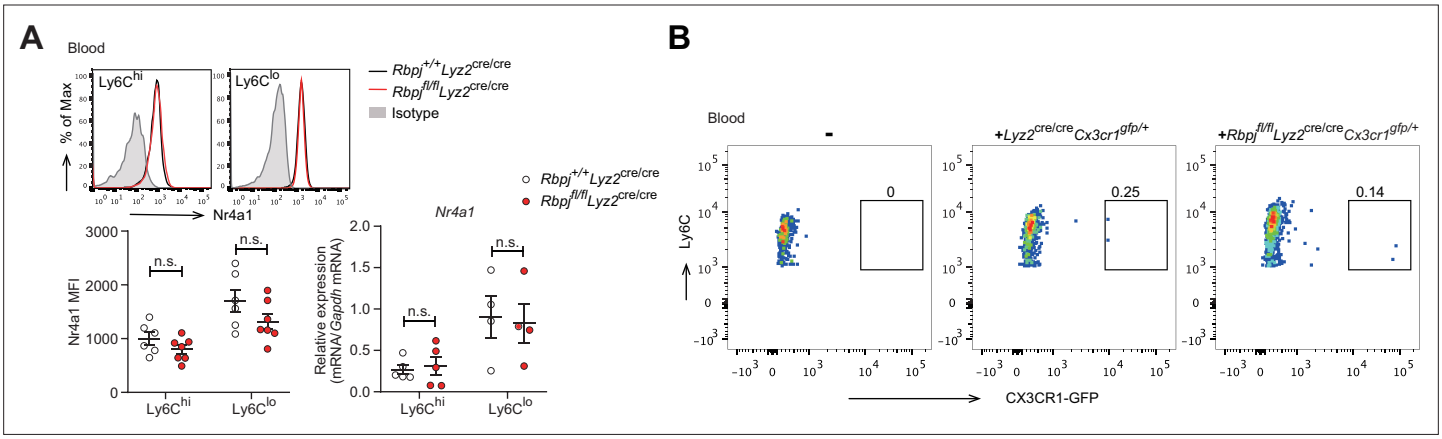

Figure 2—figure supplement 1. The conversion of Ly6C^{hi} monocyte is identical in control and RBP-J-deficient mice. (**A**) Representative FACS plots, cumulative mean fluorescence intensity (MFI) and quantitative real-time PCR (qPCR) analysis of Nr4a1 expression in control and RBP-J-deficient blood monocyte subsets. Shaded curves represent isotype control, black lines represent control mice, and red lines represent RBP-J-deficient mice. (**B**) Representative FACS plots of GFP^{+}Ly6C^{hi} monocytes in recipient. Data are pooled from two independent experiments (**A**); n ≥ 4 in each group. Data are shown as mean ± SEM; n.s., not significant (two-tailed Student's unpaired *t*-test). Each symbol represents an individual mouse.

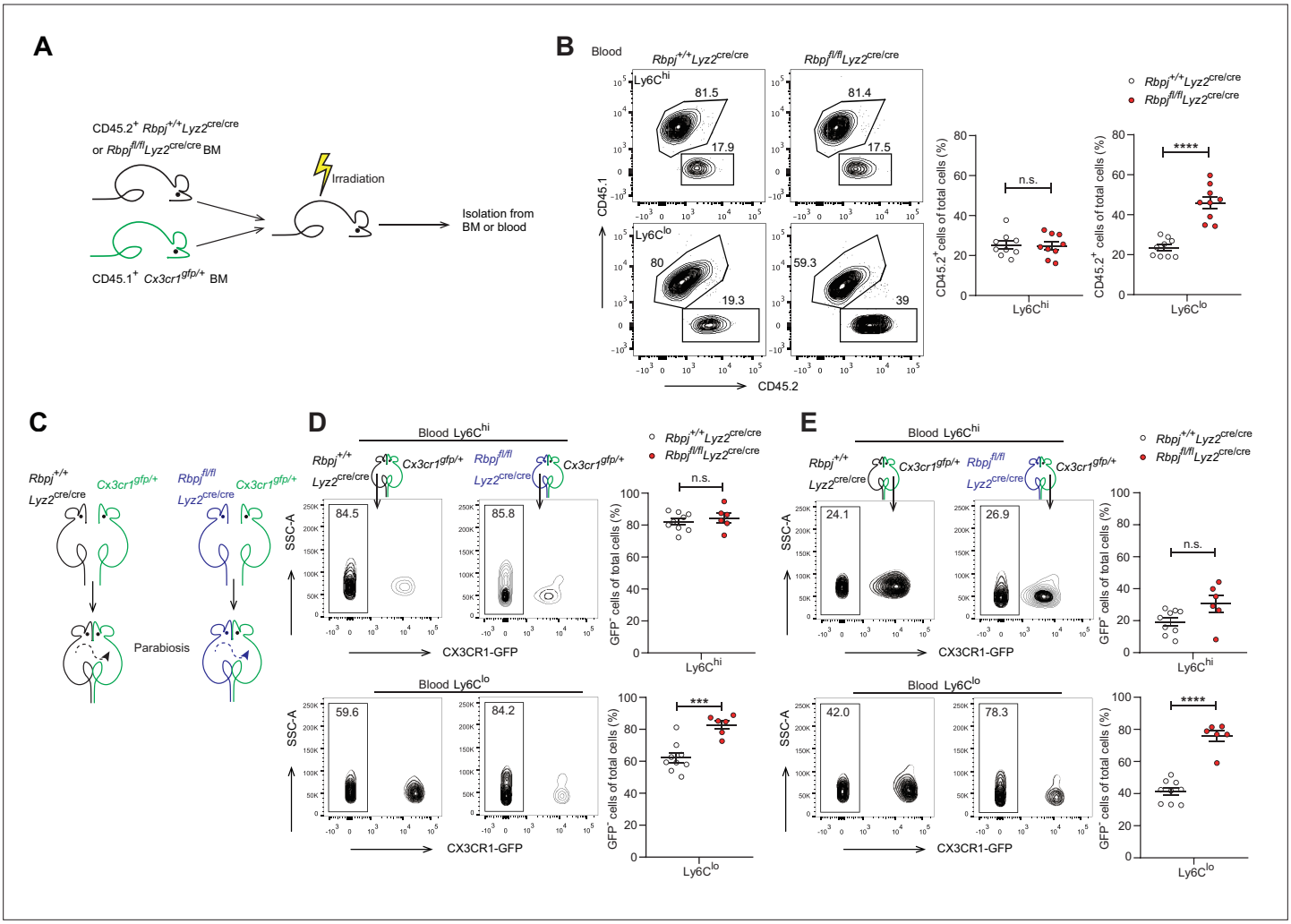

Figure 3. The role of RBP-J in blood Ly6C^{lo} monocytes is cell-intrinsic. (**A**) Cartoon depicting the bone marrow (BM) transplantation. BM recipient 6-week-old male C57BL/6 mice (CD45.2) were lethally irradiated. BM cells from donor mice (*Rbpj*$^{+/+}$*Lyz2*$^{cre/cre}$ or *Rbpj*$^{fl/fl}$*Lyz2*$^{cre/cre}$ and CD45.1, *Cx3cr1*$^{gfp/+}$) were collected and transferred into recipient mice. Mice were used after 8 wk of BM reconstitution. (**B**) Representative FACS plots (left) and cumulative data (right) quantitating the frequency of *Rbpj*$^{+/+}$*Lyz2*$^{cre/cre}$ and *Rbpj*$^{fl/fl}$*Lyz2*$^{cre/cre}$ donor cells among Ly6C^{hi} and Ly6C^{lo} monocytes in the blood of recipient mice. (**C**) Cartoon depicting the generation of *Rbpj*$^{+/+}$*Lyz2*$^{cre/cre}$ control or *Rbpj*$^{fl/fl}$*Lyz2*$^{cre/cre}$ and *Cx3cr1*$^{gfp/+}$ parabiotic pairs. (**D**) Representative FACS plots (left) and cumulative data (right) quantitating percentages of monocyte subsets derived from control or RBP-J-deficient mice in control or RBP-J-deficient mice. (**E**) Representative FACS plots (left) and cumulative data (right) quantitating percentages of monocyte subsets derived from control or RBP-J-deficient mice in *Cx3cr1*$^{gfp/+}$ mice. Data are pooled from at least two independent experiments; n ≥ 6 in each group. Data are shown as mean ± SEM; n.s., not significant; ***p<0.001; ****p<0.0001 (two-tailed Student's unpaired *t*-test). Each symbol represents an individual mouse. SSC-A, side scatter area.

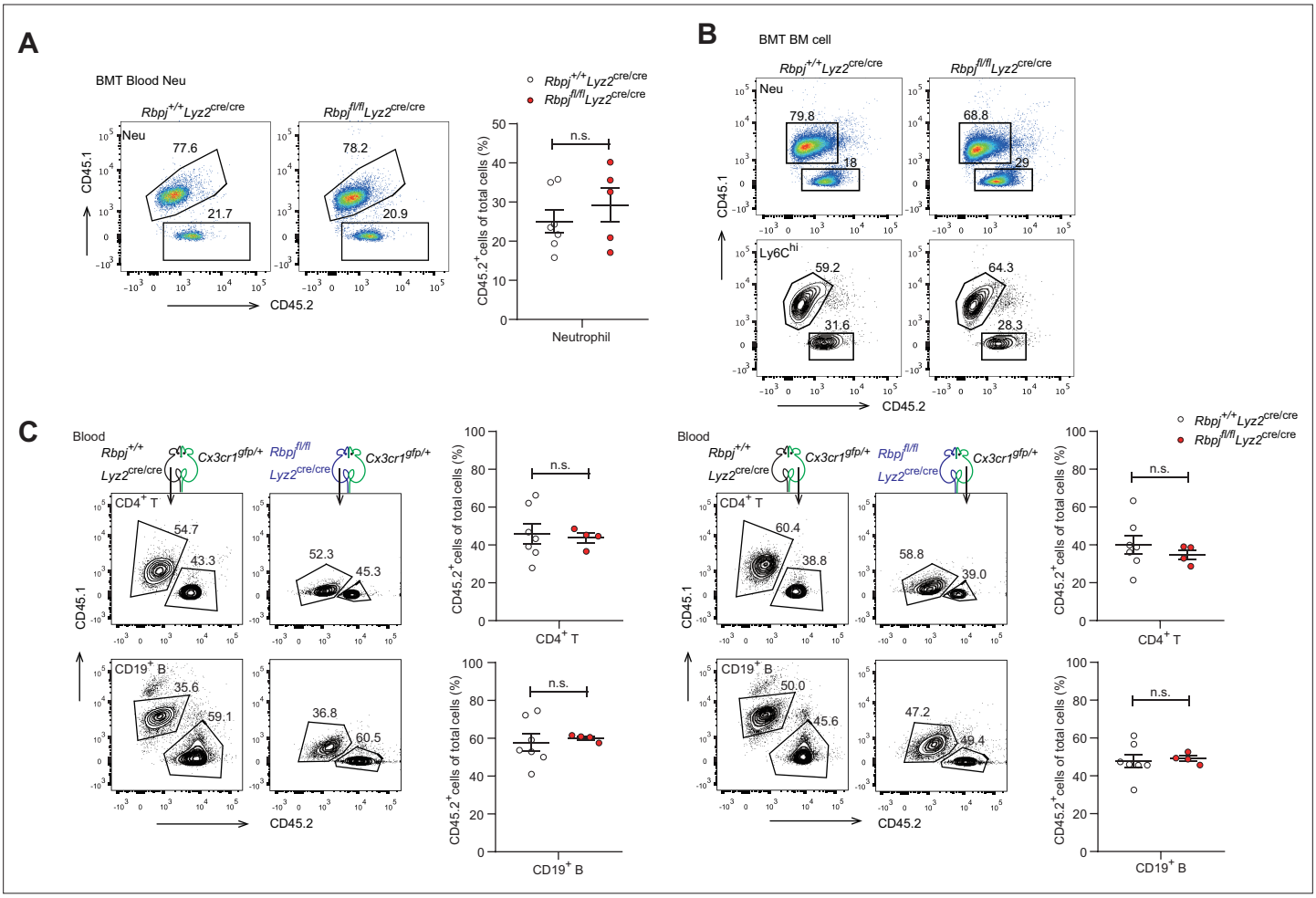

Figure 3—figure supplement 1. Cell-intrinsic requirement of RBP-J for Ly6C^{lo} monocytes maintenance. (**A**) Representative FACS plots (left) and cumulative data (right) quantitating percentages of blood neutrophils in recipient mice. (**B**) Bone marrow (BM) neutrophils and Ly6C^{hi} monocytes in recipient mice were determined by FACS. (**C**) CD4^{+} T cells and CD19^{+} B cells were analyzed by FACS in parabiotic mice. Data are pooled from at least two independent experiments (**A, C**); n ≥ 4 in each group. Data are shown as mean ± SEM; n.s., not significant (two-tailed Student's unpaired *t*-test). Each symbol represents an individual mouse.

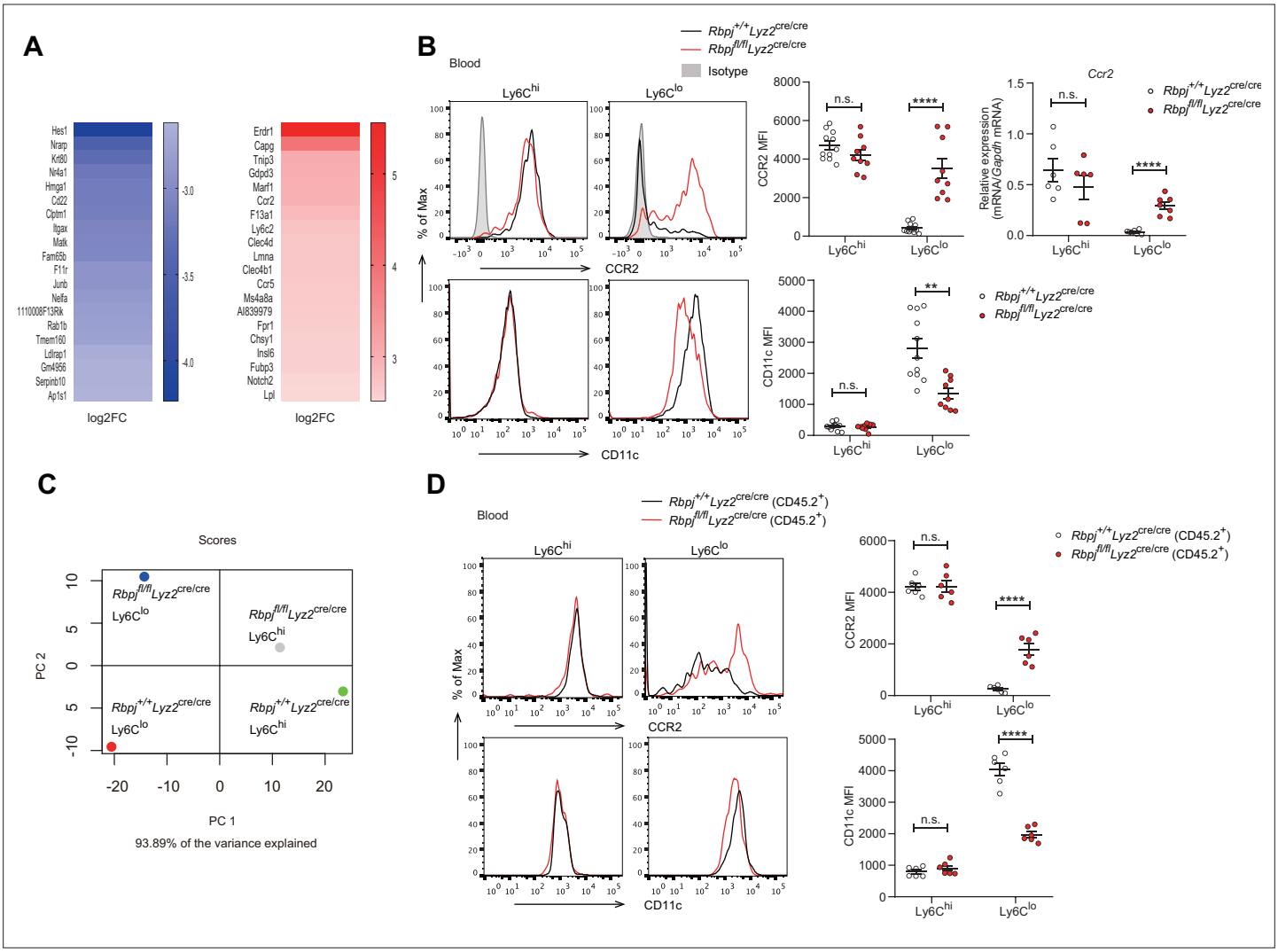

Figure 4. Phenotypic markers in Ly6C^{lo} monocytes are changed in RBP-J-deficient mice. (**A**) Heatmap of RNA-seq dataset showing the top 20 downregulated and upregulated genes in blood Ly6C^{lo} monocytes from *Rbpj*$^{fl/fl}$*Lyz2*$^{cre/cre}$ versus *Rbpj*$^{+/+}$*Lyz2*$^{cre/cre}$ control mice. Blue and red font indicates downregulated and upregulated genes in RBP-J-deficient Ly6C^{lo} monocytes respectively. (**B**) Representative FACS plots, cumulative mean fluorescence intensity (MFI), and quantitative real-time PCR (qPCR) analysis of CCR2/CD11c expression in control and RBP-J-deficient blood monocyte subsets. Shaded curves represent isotype control, black lines represent control mice, and red lines represent RBP-J-deficient mice. (**C**) Principal component analysis (PCA) of indicated cell types. (**D**) Representative FACS plots and cumulative MFI of CCR2/CD11c expression in blood monocyte subsets derived from control or RBP-J-deficient mice. Black lines represent control mice, and red lines represent RBP-J-deficient mice. Data are pooled from two independent experiments (**B, D**); n ≥ 6 in each group. Data are shown as mean ± SEM; n.s., not significant; **p<0.01; ****p<0.0001 (two-tailed Student's unpaired *t*-test). Each symbol represents an individual mouse.

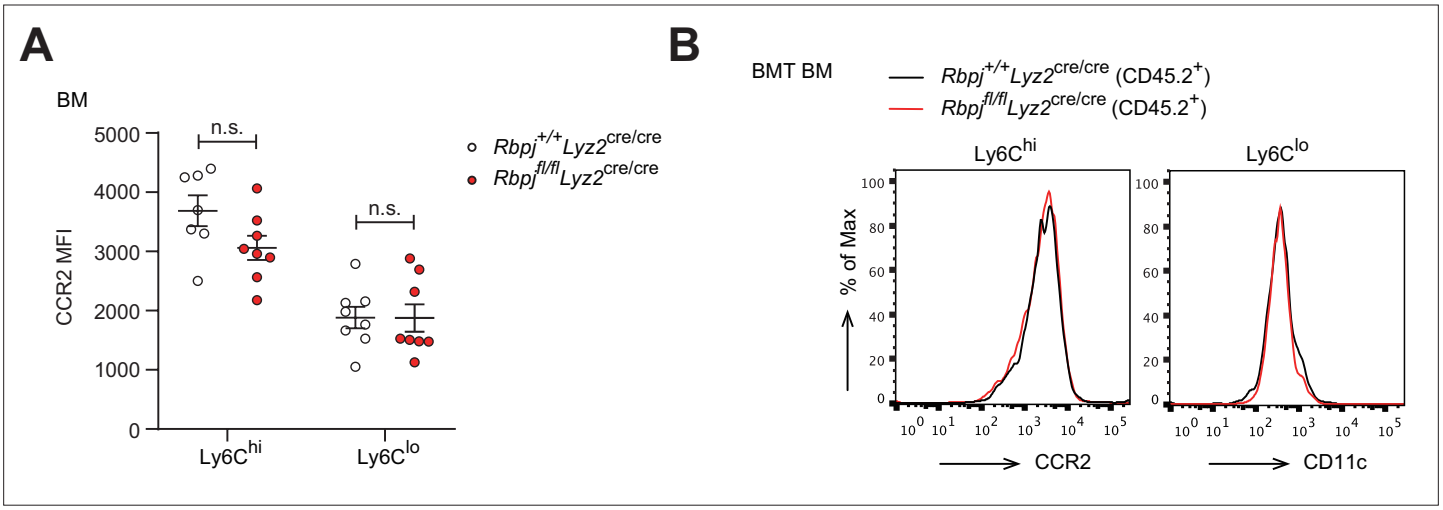

Figure 4—figure supplement 1. Normal expression of CCR2 and CD11c in bone marrow (BM) monocytes. (**A**) Cumulative mean fluorescence intensity (MFI) of CCR2 expression in BM monocyte subsets. (**B**) FACS plots of CCR2 and CD11c in BM Ly6C^{hi} and Ly6C^{lo} monocytes from control and RBP-J-deficient mice. Data are pooled from three independent experiments (**A**); n ≥ 7 in each group. Data are shown as mean ± SEM; n.s., not significant (two-tailed Student's unpaired *t*-test). Each symbol represents an individual mouse.

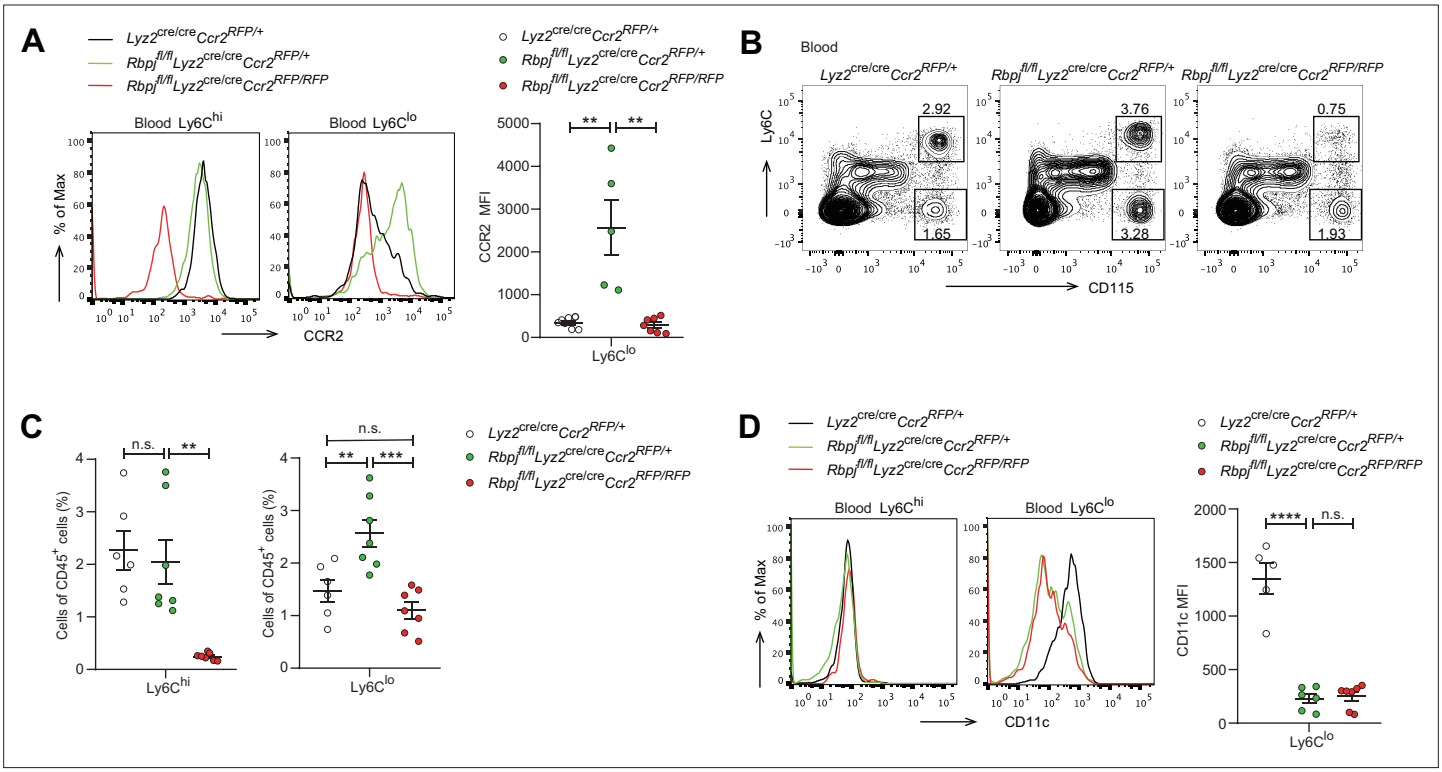

Figure 5. Blood Ly6C^{lo} monocytes are decreased in double-deficient (DKO) mice. (**A**) Representative FACS plots and cumulative mean fluorescence intensity (MFI) of CCR2 expression in *Lyz2*$^{cre/cre}$*Ccr2*$^{RFP/+}$ control, *Rbpj*$^{fl/fl}$*Lyz2*$^{cre/cre}$*Ccr2*$^{RFP/+}$ and *Rbpj*$^{fl/fl}$*Lyz2*$^{cre/cre}$*Ccr2*$^{RFP/RFP}$ (DKO) blood Ly6C^{hi} and Ly6C^{lo} monocytes are shown. (**B, C**) Blood monocyte subsets in control, RBP-J-deficient, and DKO mice were determined by FACS. Representative FACS plots (**B**) and cumulative data of cell ratio (**C**) are shown. (**D**) Representative FACS plots and cumulative MFI of CD11c expression in control, RBP-J-deficient and DKO blood Ly6C^{hi} and Ly6C^{lo} monocytes are shown. Data are pooled from at least two independent experiments; n ≥ 5 in each group. Data are shown as mean ± SEM; n.s., not significant; **p<0.01; ***p<0.001; ****p<0.0001 (two-tailed Student's unpaired *t*-test). Each symbol represents an individual mouse.

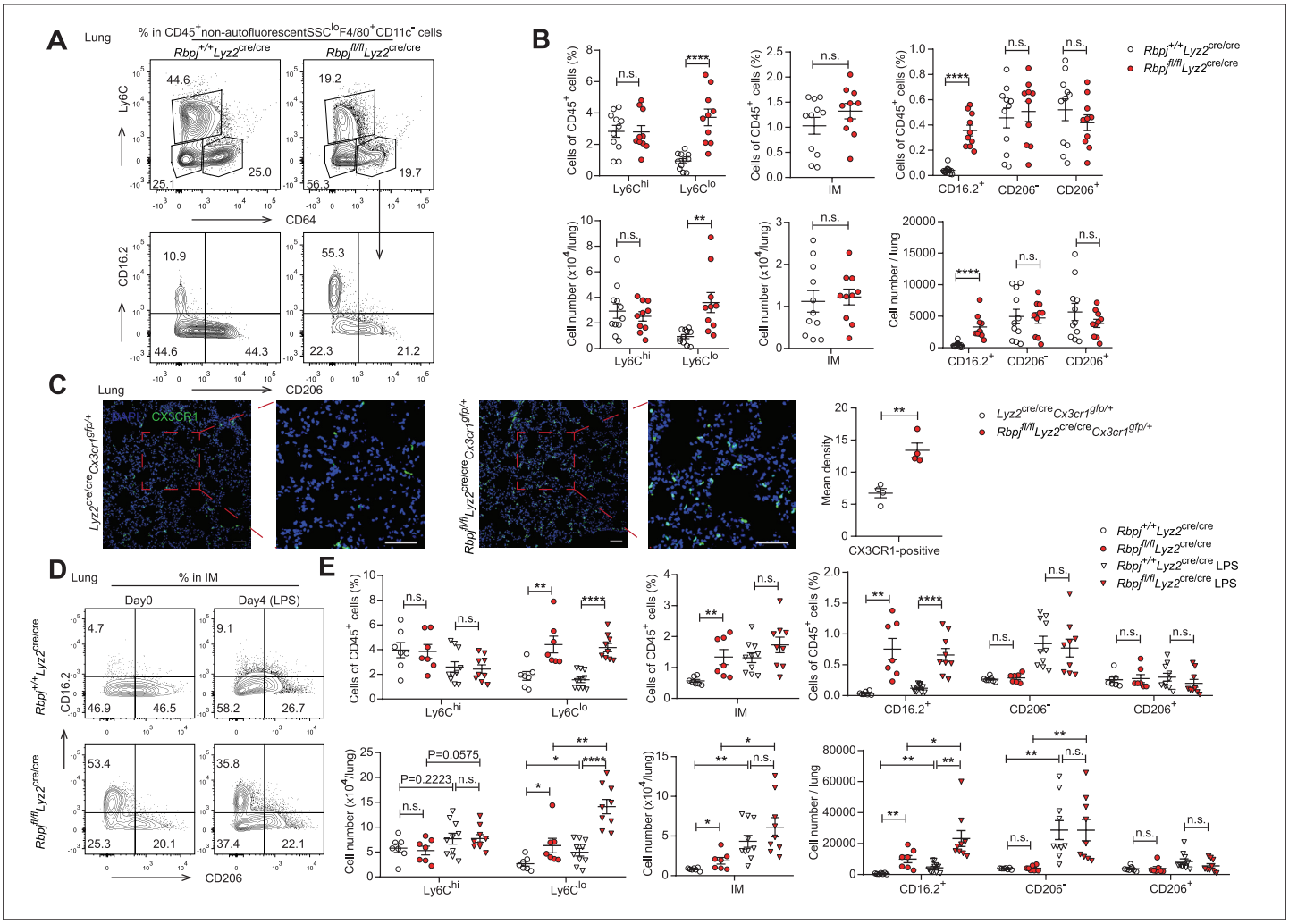

Figure 6. RBP-J-deficient mice exhibit more lung Ly6C^{lo} monocytes and CD16.2^{+} interstitial macrophages (IM). (**A, B**) indicate populations in the lungs of *Rbpj*$^{+/+}$*Lyz2*$^{cre/cre}$ and *Rbpj*$^{fl/fl}$*Lyz2*$^{cre/cre}$ mice were determined by FACS. Representative FACS plots (**A**) and cumulative data of cell ratio and absolute numbers (**B**) are shown. (**C**) Immunofluorescence staining for GFP^{+} cells in the lungs from *Lyz2*$^{cre/cre}$*Cx3cr1*$^{gfp/+}$ and *Rbpj*$^{fl/fl}$*Lyz2*$^{cre/cre}$*Cx3cr1*$^{gfp/+}$ mice (CX3CR1 [green]; DAPI [blue]). Scale bars represent 50 μm. (**D, E**) *Rbpj*$^{+/+}$*Lyz2*$^{cre/cre}$ and *Rbpj*$^{fl/fl}$*Lyz2*$^{cre/cre}$ mice were instilled intranasally with phosphate buffered saline (PBS) or PBS containing lipopolysaccharide (LPS), and lungs were harvested at the indicated time points. Representative FACS plots (**D**) and cumulative data of cell ratio and absolute numbers (**E**) are shown. Data are pooled from at least two independent experiments; n ≥ 4 in each group. Data are shown as mean ± SEM; n.s., not significant; *p<0.05; **p<0.01; ****p<0.0001 (two-tailed Student's unpaired *t*-test). Each symbol represents an individual mouse.

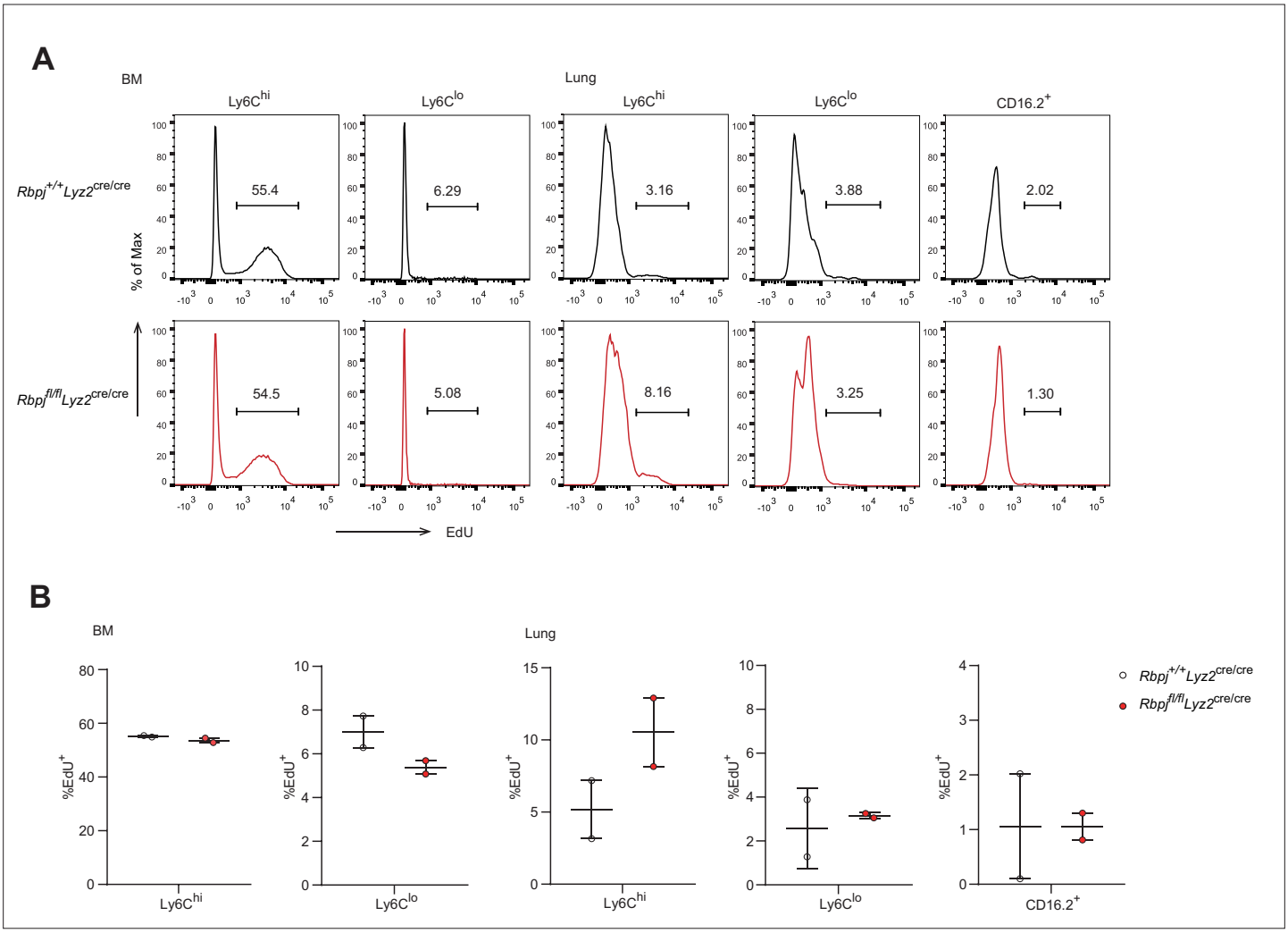

Figure 6—figure supplement 1. RBP-J is not required for turnover of lung Ly6C^{lo} monocytes and CD16.2^{+} interstitial macrophages (IM). (**A, B**) Incorporation of EdU was assessed 24 hours after injection. Bone marrow (BM) monocyte subsets were used as controls. FACS plots (**A**) and representative data (**B**) are shown. Each symbol represents an individual mouse.

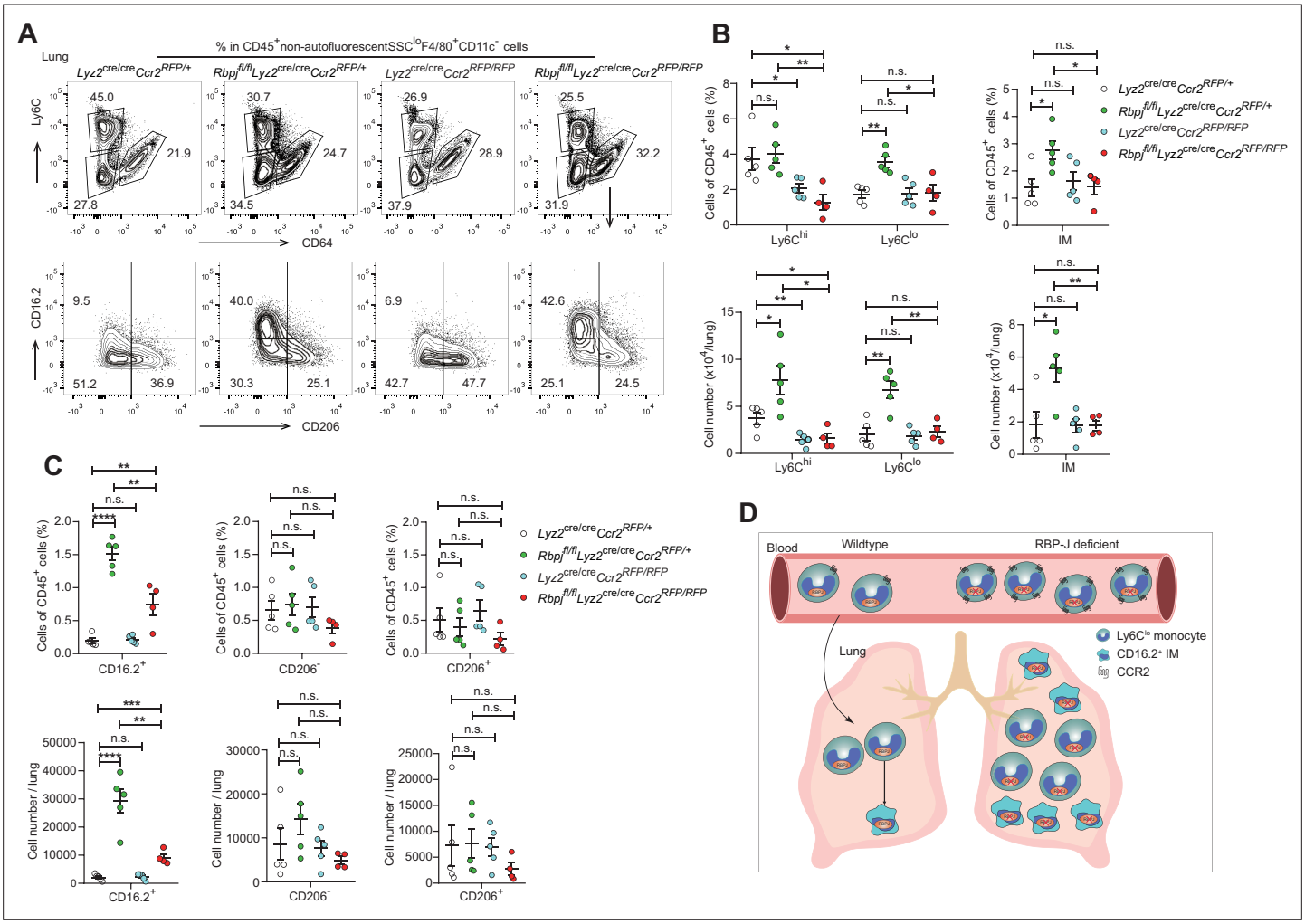

Figure 7. Double-deficient (DKO) mice lack lung Ly6C^{lo} monocytes and CD16.2^{+} interstitial macrophages (IM). (**A**) Representative FACS plots of lung monocyte and IM subsets in *Lyz2*$^{cre/cre}$*Ccr2*$^{RFP/+}$, *Rbpj*$^{fl/fl}$*Lyz2*$^{cre/cre}$*Ccr2*$^{RFP/+}$, *Lyz2*$^{cre/cre}$*Ccr2*$^{RFP/RFP}$ and *Rbpj*$^{fl/fl}$*Lyz2*$^{cre/cre}$*Ccr2*$^{RFP/RFP}$ mice. (**B, C**) Cumulative data of cell ratio and absolute numbers of monocyte (**B**) and IM (**C**) subsets. (**D**) Proposed model. RBP-J is a crucial regulator of blood Ly6C^{lo} monocytes. Mice with conditional deletion of RBP-J in myeloid cells exhibit a marked increase in blood Ly6C^{lo} monocytes, which highly express CCR2, and subsequently accumulate lung Ly6C^{lo} monocytes and CD16.2^{+} IM. Data are pooled from two independent experiments; n ≥ 4 in each group. Data are shown as mean ± SEM; n.s., not significant; *p<0.05; **p<0.01; ***p<0.001; ****p<0.0001 (two-tailed Student's unpaired *t*-test). Each symbol represents an individual mouse.